JOURNAL OF GEOPHYSICAL RESEARCH, VOL. 114, A06308, doi:10.1029/2009JA014244, 2009

Climatology of the mean total electron content derived from GPS global ionospheric maps

Libo Liu,[1] Weixing Wan,[1] Baiqi Ning,[1] and Man-Lian Zhang[1]

Received 15 March 2009; revised 11 April 2009; accepted 16 April 2009; published 17 June 2009.

[1] We analyzed 11 years' (1998–2008) worth of the total electron content (TEC) data derived at the Jet Propulsion Laboratory (JPL) from Global Positioning System (GPS) observations to investigate the overall climatological features of the ionosphere in a new way. The global ionospheric maps (GIM) of JPL TEC are averaged globally and over low-, middle-, and high-latitude ranges in the southern (northern) hemisphere and both hemispheres to identify their capability of capturing the overall features of the ionosphere. These mean TEC data show strong annual/semiannual, solar cycle, and 27-day variations. The mean TEC presents stronger solar activity sensitivity at lower-latitude bands. Moreover, the saturation effect exists in these mean TEC versus solar index $F_{10.7}$, more pronounced at low latitudes, while the mean TEC increases faster with higher solar EUV fluxes, being evident at high latitudes. The annual asymmetry (differences in June and December solstices) can be detected in the mean TEC averaged globally and at low latitudes under all solar epochs as well as at middle and high latitudes under most solar activities. The hemispheric asymmetry of the TEC in conjugate hemispheres follows the control of solar declination. Both the hemispheric differences and annual asymmetry are more marked with increasing solar activity. The annual components of the mean TEC are stronger in the southern hemisphere, and the semiannual components are of similar phases and comparable amplitudes in conjugate hemispheres, which suggest close couplings of the ionosphere in both hemispheres. Further, the mean TEC averaged in one hemisphere can reliably be used as ionospheric indices to monitor the solar activity variabilities and to capture the overall climatological features of the ionosphere over specified regions, while it should be cautioned that the mitigation of the dominant annual components with opposite phases in conjugate hemispheres leaves a significant semiannual component in the mean TEC averaged in both hemispheres, especially under low solar activity.

Citation: Liu, L., W. Wan, B. Ning, and M.-L. Zhang (2009), Climatology of the mean total electron content derived from GPS global ionospheric maps, *J. Geophys. Res.*, *114*, A06308, doi:10.1029/2009JA014244.

1. Introduction

[2] It is well known that the variations of the Earth's ionosphere are complicated and may behave quite differently from the prediction of the Chapman ionization theory. In the past decades, much effort has been conducted to draw a more detailed picture of the climatology of the Earth's ionosphere, in terms of many kinds of observations on regional and global scale [e.g., *Bailey et al.*, 2000; *Balan et al.*, 2000; *Duncan*, 1969; *Mendillo et al.*, 2005; *Oliver et al.*, 2008; *Richards*, 2001; *Rishbeth*, 1998; *Rishbeth et al.*, 2000; *Rüster and King*, 1973; *Su et al.*, 1998; *Torr and Torr*, 1973; *Torr et al.*, 1980; *West et al.*, 1997; *Wright*, 1963; *Yonezawa*, 1971; *Zhang and Holt*, 2007; *Zou et al.*, 2000]. For example, *Liu et al.* [2009] recently investigated the seasonal behaviors of daytime electron density N_e in the 200–560 km altitude range from the FORMOSAT-3/COSMIC (F3/C) radio occultation measurements during the interval from day of year (DOY) 194, 2006 to DOY 279, 2008. Their harmonic analyses provided unprecedented detail of the seasonal behaviors of global N_e at different altitudes, such as strong annual/semiannual variations in daytime N_e with distinct latitudinal and altitudinal dependency and wave-like longitudinal pattern in the equatorial regions at low solar activity (LSA). Along with the achievement in the ionospheric climatology, there are also huge progresses on the average behaviors in the thermosphere [e.g., *Bowman et al.*, 2008; *Guo et al.*, 2007; *King-Hele and Walker*, 1969; *Liu et al.*, 2005; *Qian et al.*, 2009].

[3] On the other hand, with the merit of global coverage and routine operation of Global Positioning System (GPS) derived global ionospheric maps (GIM) of vertical total electron content (TEC) [e.g., *Mannucci et al.*, 1998], *Afraimovich et al.* [2008] and *Astafyeva et al.* [2008] proposed to estimate the global electron content (GEC) of

[1]Beijing National Observatory of Space Environment, Institute of Geology and Geophysics, Chinese Academy of Sciences, Beijing, China.

0148-0227/09/2009JA014244$09.00

the ionosphere, while *Hocke* [2008, 2009] derived the global mean TEC as new parameters to track the global characteristics of the ionospheric dynamics. The principal advantage of these new parameters is that they can capture the overall ionospheric features and greatly depress local noises in the ionosphere [*Astafyeva et al.*, 2008]. Therefore, they can be served as an ionospheric index to represent the global average state of the ionosphere. Both the GEC and global mean TEC track well the solar cycle and 27-day variations of the solar irradiance and manifest a significant semiannual variation. Such new ideas can be expedient for ionospheric studies and related applications.

[4] However, we do not know the detailed behaviors of these new parameters and whether they can capture reliably the overall features of the ionosphere or not. As illustrated by *Liu et al.* [2009] and many other authors, the ionosphere has distinct latitudinal dependency. The significant semiannual variation of the global mean TEC shown by *Hocke* [2008] does not imply that the ionosphere everywhere is always varied with dominant semiannual components. If there are annual components with opposite phases in both hemispheres, the averaging processing of data from both hemispheres will weaken the annual component and mainly leave the semiannual component in GEC or global mean TEC, because of the quite similar semiannual phase in ionospheric electron density [e.g., *Liu et al.*, 2009]. We will show later, this is the case. Therefore, it may be used with caution, at least under LSA. How to utilize the merit of low local noises and at the same time to accurately capture the common regional features is a question naturally raised. Further, can we develop ionospheric indices from globally available ionospheric observations, in analog to geomagnetic indices, to reliably indicate the state of the ionosphere for monitoring, nowcasting, and forecasting of the ionospheric weather, and even for related studies? Therefore, the first thing deserved to be explored is the behaviors of these mean TEC estimated globally and over different latitude ranges.

[5] In this paper, we investigate these mean TEC averaged respectively globally as well as over low-, middle-, and high-latitude ranges in one hemisphere or both hemispheres, to elucidate the responses of the ionosphere to solar cycle and solar rotation variations and to provide more detailed features of annual variations of these mean TEC over different latitude bands, including annual/semiannual features and hemispheric and annual asymmetries as well under different solar epochs. The most important findings are that all these mean TEC can reliably track the solar activity variabilities with noises greatly decreased; and only these TEC averaged in one (southern or northern) hemisphere can be used as ionospheric indices to reliably capture the overall annual/semiannual features of the ionosphere over specified regions, while the TEC averaged in both hemispheres may possibly provide distorted information on the annual/semiannual variations, especially at LSA.

2. Mean TEC at Different Latitude Bands

[6] Global ionospheric maps (GIMs) of the GPS-derived TEC have been routinely produced at five analysis centers on the basis of measurements from the international network of GPS receivers. In this work, we used the GIM TEC generated at Jet Propulsion Laboratory (JPL) on an hourly and daily basis using data from up to 100 GPS sites of the IGS and other institutions since 1998 [e.g., *Mannucci et al.*, 1998; *Iijima et al.*, 1999]. The global maps of vertical TEC are modeled in a solar-geomagnetic reference frame using bicubic splines on a spherical grid. A Kalman filter is used to solve simultaneously for TEC and instrumental biases on the grids. A detailed description of the TEC deriving procedure is given by *Mannucci et al.* [1998]. The estimated TEC in geographic coordinate system and other information are available from the Web site ftp://cddis.gsfc.nasa.gov/gps/products/ionex/ in the form of IONosphere map EXchange format (IONEX) files with a temporal resolution of 2 h and a spatial resolution of 5° in longitude and 2.5° in latitude.

[7] We calculated the global mean TEC from JPL GIM in the similar way of *Afraimovich et al.* [2008], *Astafyeva et al.* [2008], and *Hocke* [2008]. The GEC of *Afraimovich et al.* [2008] and *Astafyeva et al.* [2008] can easily be converted into the global mean TEC by normalizing the GEC with the area of the Earth at the ionospheric shell altitude, and the global mean TEC can also be converted into GEC by multiplying the summation area. Moreover, the unit of the mean TEC is similar to that of TEC (in TECu, where 1 TECu = 10^{16} electrons/m^2), and the mean TEC can be understood as an idealized ionosphere in which TEC is uniformly distributed and, as a whole, has the same electron content as the actual ionosphere, therefore the global mean TEC should represent the global characteristics of the ionosphere.

[8] To capture the general behaviors of the TEC over different latitude ranges, we further evaluated the mean TEC ($\overline{TEC}$) averaged in the northern (southern) hemisphere and both hemispheres as well over latitudinal ranges at low latitude (0°–25°), middle latitude (25°–55°), and high latitude (>55°). This attempt is analog to the proposal of different geomagnetic indices (Dst, Kp and AE, etc.). In the following, we denote $\overline{TEC}_l^S$ for the mean TEC averaged at low latitudes (denoted by the subscript "*l*") in the southern hemisphere (denoted by the superscript "*S*"), and the other symbols and their meanings are listed in Table 1. The subscripts *l*, *m*, and *h* of those symbols stand for low, middle, and high latitude, while the superscripts *N*, *S*, and *G* stand for the northern, southern, and both hemispheres, respectively. We will see later, these mean TEC evaluated over specified latitude ranges can be considered as ionospheric indices to provide general information of the ionosphere globally or over specified latitude ranges. The error budget of the mean TEC has been discussed by *Astafyeva et al.* [2008]. They reported that the relative errors of these mean TEC are much smaller than those of the TEC in GIM cells.

[9] Information of the solar variability, here mainly referred to the solar cycle and 27-day variations, was obtained from the daily values of 10.7 cm solar radio flux, $F_{10.7}$ and the solar extreme ultraviolet (EUV) fluxes in 0.1–50 nm wavelength ranges from the Solar EUV Monitor (SEM) spectrometer aboard on the Solar Heliospheric Observatory (SOHO). Since 1996, solar EUV fluxes in 26–34 nm and 0.1–50 nm wavelength ranges were continuously monitored by SOHO/SEM [*Judge et al.*, 1998], which provide direct information of solar EUV variability.

Table 1. Symbols Used in This Article and Their Meaning

Symbol	Meaning
$\overline{TEC}_l^S$	TEC averaged over southern low latitudes (0°–25°S)
$\overline{TEC}_l^N$	TEC averaged over northern low latitudes (0°–25°N)
$\overline{TEC}_l^G$	TEC averaged over global low latitudes (25°N–25°S)
$\overline{TEC}_m^S$	TEC averaged over southern middle latitudes (25°S–55°S)
$\overline{TEC}_m^N$	TEC averaged over northern middle latitudes (25°N–55°N)
$\overline{TEC}_m^G$	TEC averaged over global middle latitudes (25°N–55°N, 25°S–55°S)
$\overline{TEC}_h^S$	TEC averaged over southern high latitudes (55°S–87.5°S)
$\overline{TEC}_h^N$	TEC averaged over northern high latitudes (55°N–87.5°N)
$\overline{TEC}_h^G$	TEC averaged at global high latitudes (55°N–87.5°N, 55°S–87.5°S)
$\overline{TEC}^S$	TEC averaged in the southern hemisphere (0°–87.5°S)
$\overline{TEC}^N$	TEC averaged in the northern hemisphere (0°–87.5°N)
$\overline{TEC}^G$	TEC averaged over global (87.5°N–87.5°S)

At the same time, $F_{10.7}$ is often used as a standard proxy for solar activity. In this paper, we adopt the daily average values of EUV in 0.1–50 nm wavelength ranges from SOHO/SEM and the adjusted values of $F_{10.7}$ which are provided at the SPIDR Web site in accord with the work of *Liu et al.* [2006, 2007a], since different $F_{10.7}$ values (the observed, adjusted and absolute values provided by the U.S. National Geophysical Data Center) do not greatly affect our conclusions on ionospheric solar cycle effect, but it may have slight consequences when we use it to explore the solar rotation (27-day) effects of the ionosphere.

3. Results and Discussions

3.1. General Perspective of the Mean TEC Averaged in Both Hemispheres

[10] Figure 1 shows the time series of $F_{10.7}$, daily geomagnetic index Ap, SOHO/SEM EUV in 0.1–50 nm wavelength ranges since 1996, and the mean TEC ($\overline{TEC}_l^G$, $\overline{TEC}_m^G$, $\overline{TEC}_h^G$, and $\overline{TEC}^G$) which were averaged in both hemispheres at low latitudes (25°N–25°S), middle latitudes (25°N–55°N and 25°S–55°S), high latitudes (>55°N and >55°S), and global during the years 1998 to 2008. The data of these mean TEC are shown with diamonds when the values of Ap exceeded 30 nT. The unit of EUV fluxes is 10^9 photons cm^{-2} s^{-1} and that of $F_{10.7}$ is in solar flux unit (1 sfu = 10^{-22} W m^{-2} Hz^{-1}). The thick lines denote the corresponding values moving averaged with a 1-year window. The technique of applying a moving average can suppress the short-term variations.

[11] As illustrated in Figure 1, the daily values of the mean TEC ($\overline{TEC}_l^G$, $\overline{TEC}_m^G$, $\overline{TEC}_h^G$, and $\overline{TEC}^G$) present variations with different time scales. An initial analysis of the global mean TEC has been given by *Hocke* [2008] and in a reply by *Hocke* [2009]. The variations of these mean TEC denoted by thick lines follow those of $F_{10.7}$ and EUV. With increasing (decreasing) solar activity, these mean TEC tend to increase (decrease). A consistent pattern that can also be detected is that all mean TEC, solar EUV and $F_{10.7}$ have a trough in 2001 and two broad peaks in 2000 and 2002–2003, respectively. An analysis of the amplitude spectra of GEC has been conducted by *Afraimovich et al.* [2008] with a wavelet method. Moreover, in the short-term variation range of these mean TEC, the rough 27-day variations are significant and closely follow the solar rotation variations in $F_{10.7}$ and EUV. This indicates the strong forcing of solar irradiance to the ionosphere. The solar rotation variations in these mean TEC in solar cycle 23 are more evident and regular during the ascending and descending periods than during the solar maximum and minimum years. The reason for this feature in GEC has been discussed by *Afraimovich et al.* [2008]. They proposed that it was related with the dynamics of the active region formation on the Sun's surface during different phases of a solar cycle.

[12] Accompanying with the solar cycle and solar rotation variations, there are significant annual/semiannual components in these mean TEC averaged in both hemispheres, with minima in solstices and maxima near equinoxes at all solar epochs. *Afraimovich et al.* [2008] and *Hocke* [2008] have mentioned the dominated semiannual component in global mean TEC and GEC. As illustrated in Figure 1, the semiannual modulation is more obvious in the mean TEC averaged globally and at low latitudes than at middle and high latitudes. We addressed here the fact that the semiannual component can be found in these mean TEC averaged in both hemispheres at different solar epochs and becomes most pronounced around the solar maximum period.

3.2. Annual Variations of the Mean TEC in the Southern and Northern Hemispheres

[13] Figure 2 shows the daily mean TEC averaged at three latitude bands in the southern hemisphere (denoted by red curves) and in the northern hemisphere (blue curves) as a function of day of year (DOY) in 2000 to 2008. Note that to make the data more discernable, in all plots of Figure 2 $\overline{TEC}_l^S$ and $\overline{TEC}_l^N$ have been elevated 20 TECu, and $\overline{TEC}_m^S$ and $\overline{TEC}_m^N$ with 10 TECu larger. In each plot, the dashed line denotes the fitting data in the southern hemisphere and the thick line for the northern hemisphere.

[14] The annual/semiannual components are most dominant in the annual variation of the ionosphere [e.g., *Fukao et al.*, 1991; *Kawamura et al.*, 2002; *Mayr and Mahajan*, 1971; *Meza and Natali*, 2008; *Zhao et al.*, 2005]. Therefore, the annual variations of the mean TEC ($\overline{TEC}$) can be represented as a combination of the components of annual (A_{annual}), semiannual ($A_{semiannual}$) and annual mean (A_0):

$$\overline{TEC}(d) = A_0 + A_{annual} + A_{semiannual} + \varepsilon, \quad (1)$$

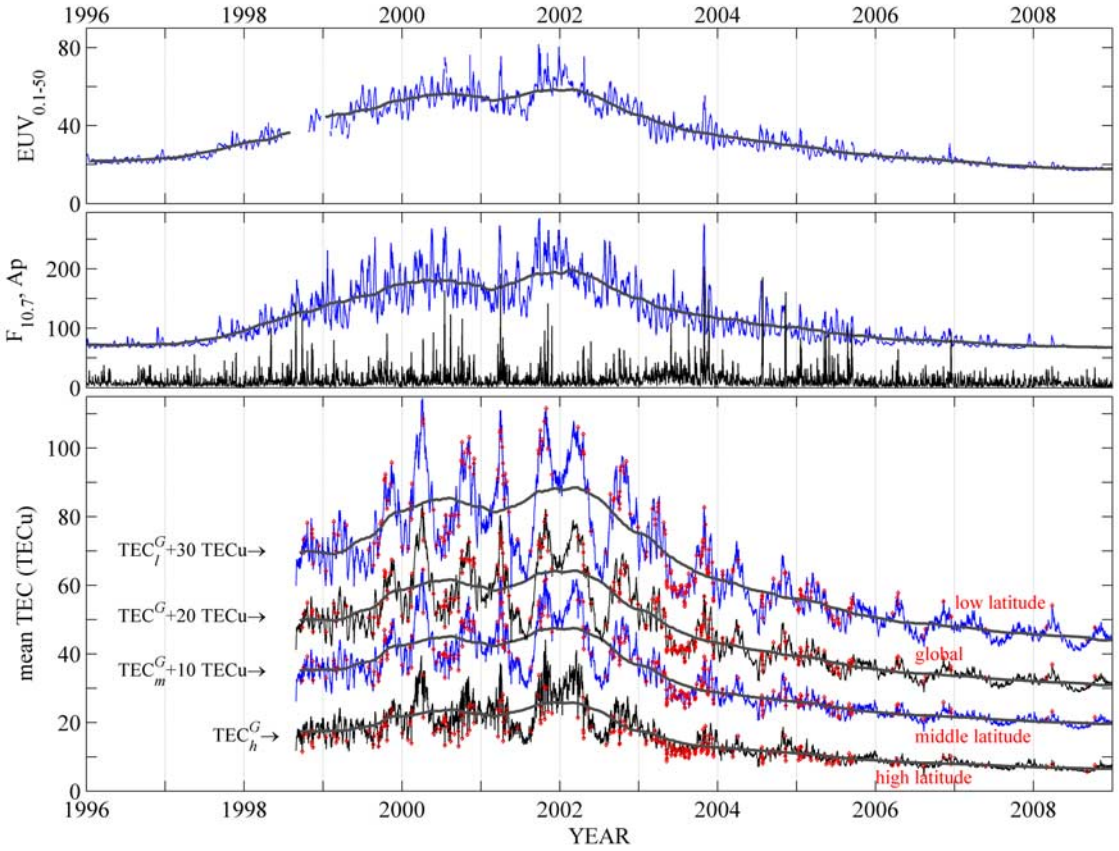

Figure 1. (top) The daily averaged SOHO/SEM EUV fluxes (in units of 10^9 photons cm^{-2} s^{-1}) at the 0.1–50 nm wavelength band, (middle) 10.7 cm solar radio flux index $F_{10.7}$ (in solar flux units; 1 sfu = 10^{-22} W m^{-2} Hz^{-1}) and daily geomagnetic index Ap, and (bottom) the mean TEC values of GPS-derived JPL global ionospheric maps (GIM), which are averaged at low latitudes (25°N–25°S), middle latitudes (55°N–25°N, and 25°S–55°S), high latitudes (latitudes poleward of 55°N and 55°S), and global of both hemispheres from 1996 to 2008, respectively. The subscripts *l*, *m*, and *h* stand for low, middle, and high latitude, while the superscript *G* stands for both hemispheres. The heavy solid lines denote the 1-year moving mean series. Ticks of year are on 1 January of the years. Note that in Figure 1 (bottom), the values of the mean TEC have been shifted 30 TEC units (TECu, 1 TECu = 1×10^{16} el m^{-2}) for low latitudes, 20 TECu for all latitudes, and 10 TECu for middle latitudes. The diamond points illustrate the situations when the value of daily Ap is higher than 30 nT.

where d is DOY, ε is the corresponding residual term, and

$$A_{annual} = C_{12}\cos\frac{2\pi d}{365.25} + S_{12}\sin\frac{2\pi d}{365.25} = A_{12}\cos\frac{2\pi d}{365.25}(d-\varphi_{12}),$$

$$A_{semiannual} = C_6\cos\frac{4\pi d}{365.25} + S_6\sin\frac{4\pi d}{365.25} = A_6\cos\frac{4\pi}{365.25}(d-\varphi_6).$$

A_{12} and A_6 are the amplitudes of the annual and semiannual components, and φ_{12} and φ_6 are the corresponding phases in units of day of year.

[15] Figure 3 plots the amplitudes and phases of the annual/semiannual components of these mean TEC averaged in the northern hemisphere (blue curves) and in the southern hemisphere (red curves) derived from the data in terms of harmonic analyses with a moving window of 1 year according to equation (1).

[16] One can see from Figures 2 and 3 that the annual variations of these mean TEC are modulated by the levels of solar activity and have latitudinal and hemispheric differences. Similar to these mean TEC averaged in both hemispheres (Figure 1), the semiannual components in these mean TEC averaged in the southern (northern) hemisphere peak near equinoxes and become more obvious in higher solar activity years. Moreover, the semiannual amplitudes are highest at low latitudes, weaker at middle latitudes, and smallest at high latitudes. It is well known that the thermospheric neutral density also shows strong semiannual variations [see, e.g., *Bowman et al.*, 2008; *Fuller-Rowell*, 1998; *Guo et al.*, 2007; *Qian et al.*, 2009]. Many hypotheses have been proposed as the mechanisms for the semiannual variations in the ionosphere and in the thermosphere [*Fuller-Rowell*, 1998; *Millward et al.*, 1996; *Rüster and King*, 1973;

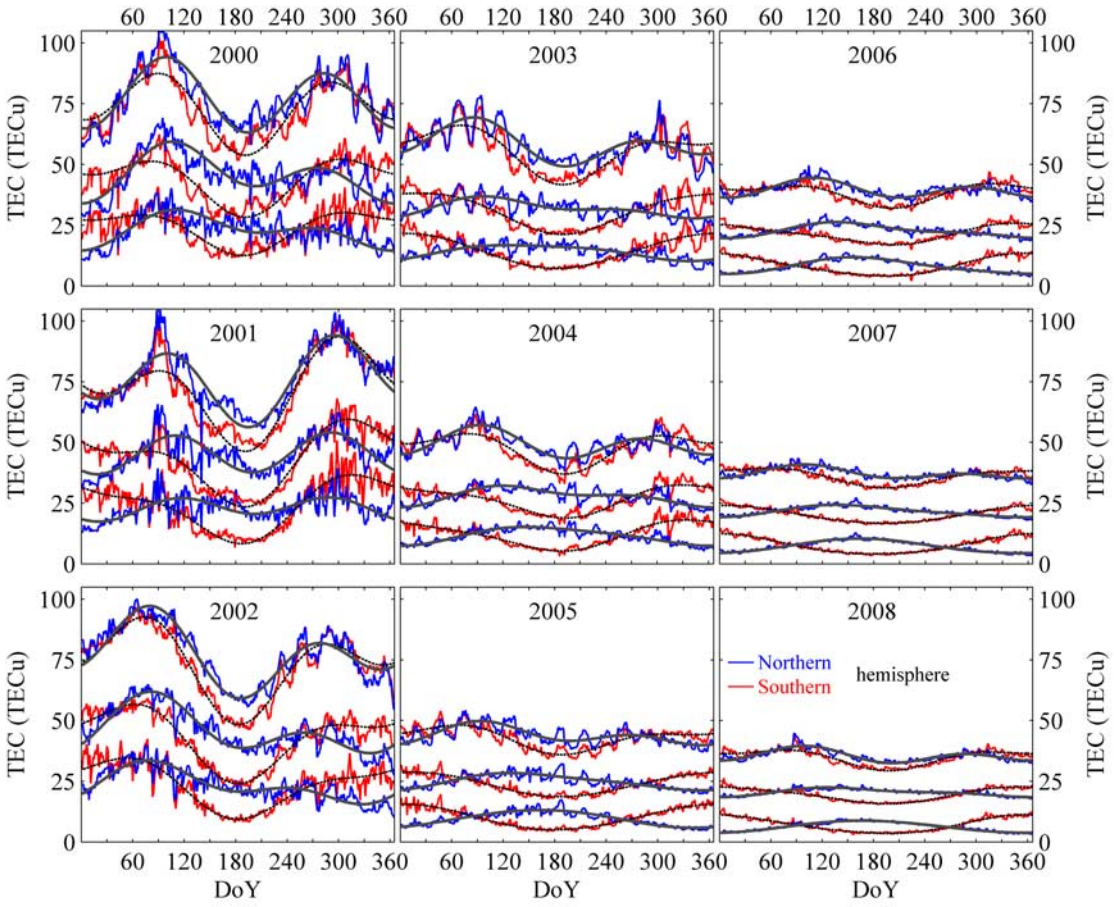

Figure 2. The daily mean TEC of GPS-derived JPL global ionospheric maps (GIM), which are averaged at low-latitude (25°–0°), middle-latitude (55°–25°), and high-latitude (latitude higher than 55°) bands in the southern (red curve) and northern (blue curve) hemispheres in the years 2000 to 2008. Superimposed dashed curves and heavy solid lines denote the corresponding regression results, using the annual harmonics (annual, semiannual, terannual, and mean terms). The four-digit number (e.g., 2000 at the top left) denotes the year of data. Note that the curves from the top to the bottom are in the order of the low-, middle-, and high-latitude bands, and the mean TEC values have been shifted 20 TECu larger for low latitude and 10 TECu for middle latitude to plot them together and to make them discernible.

Yonezawa, 1971; *Qian et al.*, 2009]. It is interesting that the overall latitudinal structure of the ionospheric semiannual feature is quite different from that in the thermosphere as revealed in the observations [e.g., *Guo et al.*, 2007] and empirical models (such as the MSIS model [e.g., *Hedin*, 1991]). For example, in terms of the data derived from the CHAMP observations, *Guo et al.* [2007] revealed that the semiannual amplitudes of the total neutral density normalized at 400 km altitude have varying latitudinal dependencies in different years, being very weak latitudinal structures in 2004 and larger amplitudes at northern middle and high latitudes in 2003 and 2005. Of course, the difference is not only limited to the CHAMP observations. In contrast, our results and many other investigations [e.g., *Bailey et al.*, 2000; *Ma et al.*, 2003; *Su et al.*, 1998; *Liu et al.*, 2009; *Yu et al.*, 2004; *Zou et al.*, 2000] indicate that the semiannual amplitude in the ionosphere is always largest at low latitudes. The inconsistency between the ionosphere and the thermosphere on the semiannual latitudinal structure implies that the semiannual variation in the ionosphere is not absolutely attributed by the variation of the neutral density, and possibly contributed from other factors or processes [*Ma et al.*, 2003]. Further, the quite similar features of the semiannual phases and amplitudes in both hemispheres suggest close couplings between both hemispheres, indicating the key role of the dynamic and electrodynamical processes in the ionospheric semiannual variation. To explain the main feature of the semiannual variations in the ionosphere at low latitude, *Ma et al.* [2003] proposed that the semiannual variation of the diurnal tide modulates the variations of equatorial electric fields and electrojet via the wind dynamo processes, and further controls the ionosphere through the fountain effect.

[17] The semiannual amplitudes are larger in the years 2000–2002, and they become much smaller before 2000 and after 2002. At middle and high latitudes, the annual component exceeds the semiannual component in the southern hemisphere during the entire period we considered and at most times in the northern hemisphere except in

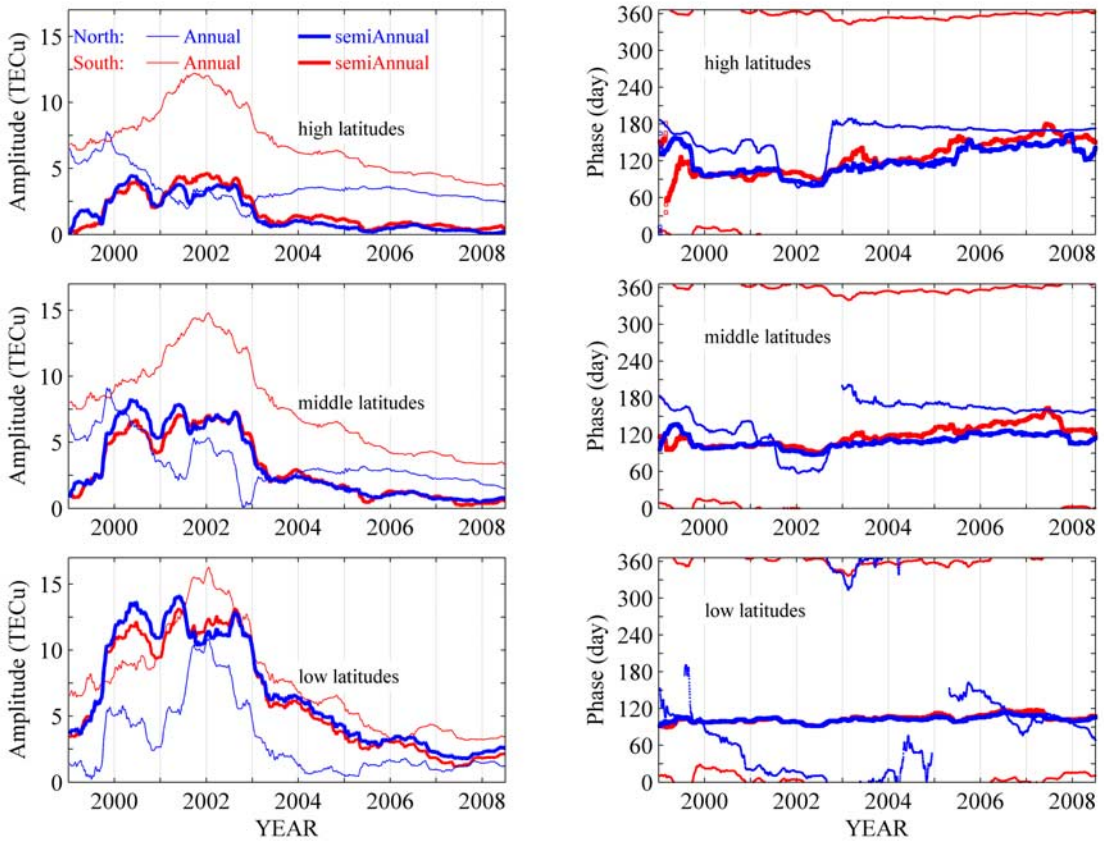

Figure 3. The amplitudes (in TECu) and phases (in days) of the annual and semiannual components of the mean TEC averaged in the southern (red curve) and northern (blue curve) hemispheres at low latitudes (25°–0°), middle latitudes (55°–25°), and high latitudes (latitude higher than 55°) in the years 1999 to 2008. The amplitudes and phases at the different latitude bands are derived from the corresponding mean TEC in a moving window of 1 year, using the annual harmonics including the terms of annual, semiannual, terannual, and annual mean. In each plot the semiannual component is indicated by the heavy curve, and the annual component is indicated by thin curve. Ticks of year are on 1 January of the years.

2000–2002, when the semiannual amplitude is larger than the annual amplitude. At low latitudes, the semiannual component of $\overline{TEC}_l^S$ and $\overline{TEC}_l^N$, becomes most pronounced, compared to that at middle and high latitudes. The semiannual component of the mean TEC in the southern low latitude is comparable with the annual component in 2000–2002 and weaker than the annual component in other years; while in the northern hemisphere the semiannual component dominates over the annual component all the years.

[18] As depicted in the right-hand plots of Figure 3, the phase of the annual variations in the southern hemisphere appears in local summer, varying little with latitude and solar activity. In contrast, the annual phase changes with solar activity in the northern hemisphere. An interesting point is that during the high solar activity years, the annual phase at middle and high latitudes in the northern hemisphere shifts earlier from the June solstice. This feature is quite similar to that in the DMSP total plasma density [*Liu et al.*, 2007b] at 840 km altitude. The annual phases of $\overline{TEC}_l^N$ are shifted from vernal equinox to the northern winter solstice in 2000–2004.

[19] In general, these mean TEC averaged in one hemisphere at different latitude bands show consistent features of annual variations in the ionospheric *F* region and TEC in previous investigations [e.g., *Titheridge and Buonsanto*, 1983; *Liu et al.*, 2009; *Yonezawa*, 1971; *Zhao et al.*, 2007]. For example, the left-hand plots of Figure 3 shows that the annual amplitudes of these mean TEC over different latitude ranges are larger in the southern hemisphere than in the northern hemisphere. *Liu et al.* [2009] reported that the peak electron density (NmF2) derived from the Formosat-3/COSIC radio occultation observations at LSA shows a stronger annual component in the southern hemisphere than in the northern hemisphere. Thus it identifies that these mean TEC can capture the overall features of the ionosphere over the specified regions. Further, the semiannual component at all latitude ranges has similar phases and comparable amplitudes in both hemispheres. The global mean TEC shows strong semiannual variations in solar minimum years (2006–2008), when the annual variation dominates in the ionosphere, especially at middle and low latitudes. Therefore, although the global mean TEC depicts strong semiannual variations even at LSA, it does not imply that the ionosphere is always dominated with semiannual components. The semiannual feature in the global mean TEC at LSA is due to mitigation effect of annual variations with

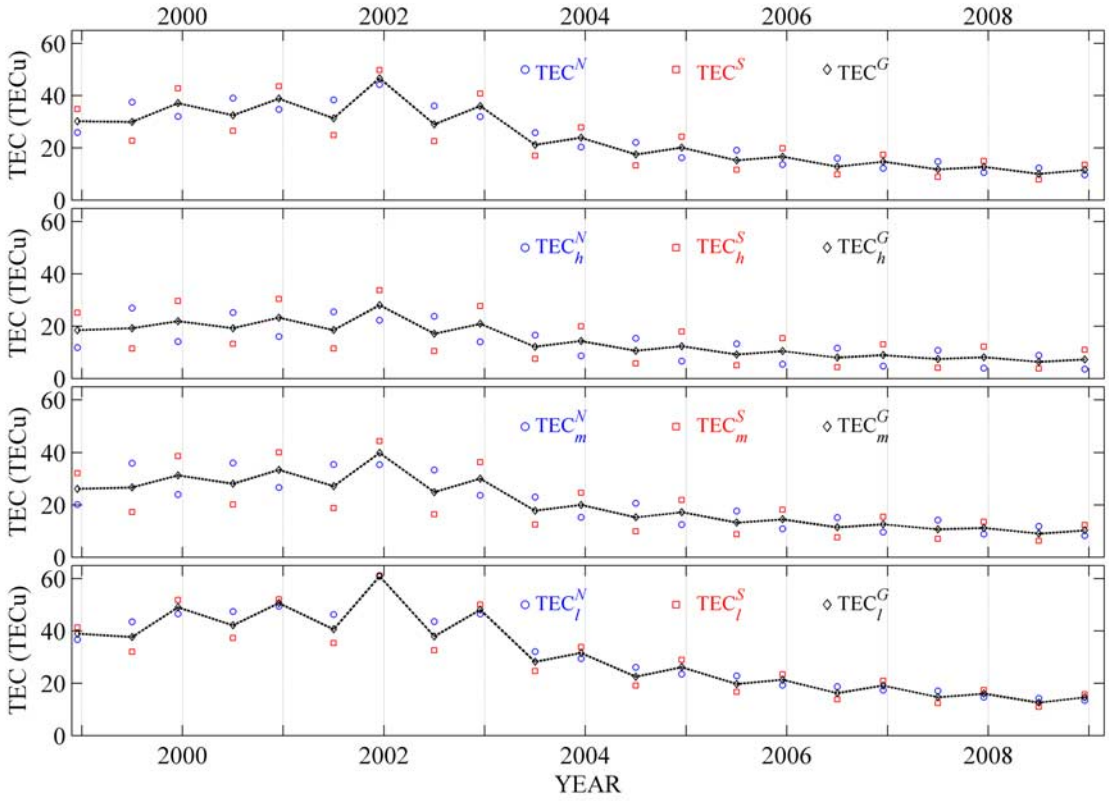

Figure 4. Monthly mean values of the TEC averaged in June and December months during the years 1999 to 2008 at all latitudes (0°–87.5°), high latitudes (latitude higher than 55°), middle latitudes (55°–25°), and low latitudes (25°–0°). The circles denote those in the northern hemisphere, squares are for those in the southern hemisphere, and diamonds are for those averaged in both hemispheres. The subscripts *l*, *m*, and *h* stand for low, middle, and high latitude, while the superscripts *N*, *S*, and *G* stand for the northern, southern, and both hemispheres. Ticks of year are on 1 January of the years.

opposite phases in both hemispheres. Therefore, it should be cautioned that these mean TEC averaged in both hemispheres are not suitable for indicating the annual and semiannual variations in the ionosphere; in contrast, these TEC averaged in one hemisphere can reliably capture the overall features of the ionospheric annual/semiannual variations.

3.3. Mean TEC in Solstice Seasons

[20] The ionosphere at solstices is an interesting issue [*Duncan*, 1969; *Fatkullin*, 1973; *Liu et al.*, 2007b; *Mendillo et al.*, 2005; *Rishbeth*, 1998; *Rishbeth et al.*, 2000; *Rishbeth and Müller-Wodarg*, 2006; *Torr et al.*, 1980; *Torr and Torr*, 1973; *Wright*, 1963; *Zeng et al.*, 2008]. There is the well-known annual asymmetry, characterized by on global average higher electron densities near the December solstice than near the June solstice. This feature was also found in TEC, NmF2, and the topside ionospheric electron density [*Bailey et al.*, 2000; *Liu et al.*, 2007b; *Mendillo et al.*, 2005; *Rishbeth and Müller-Wodarg*, 2006; *Su et al.*, 1998; *Zeng et al.*, 2008]. How to explain the annual asymmetry is still an open question in ionospheric physics [*Rishbeth*, 1998]. Possible contributions may come from the geomagnetic field configuration, the Sun-Earth distance, and lower atmospheric tidal forcing [*Zeng et al.*, 2008].

[21] To identify the evolution of these mean TEC near solstices, we plotted in Figure 4 the monthly mean TEC in June and December. The circles denote the TEC values averaged in the northern hemisphere, squares for those in the southern hemisphere, and diamonds for those averaged in both hemispheres.

[22] As shown in Figure 4, in the southern hemisphere, the monthly values of the mean TEC ($\overline{TEC}_l^S$, $\overline{TEC}_m^S$, $\overline{TEC}_h^S$ and $\overline{TEC}^S$) are higher in December than in June during the years 1999 to 2008; the behaviors in the northern hemisphere do not show a consistent feature. The values of $\overline{TEC}_h^N$ are always higher in June than in December. In contrast, $\overline{TEC}_m^N$ and $\overline{TEC}_l^N$ are relatively complicated. Compared to that in December, $\overline{TEC}_l^N$ in June has higher values in 1999 and 2000, lower values in the years 2001, 2002, and 2008, and a decline trend in other years partly due to the solar activity variations as illustrated in Figure 1. The monthly values of $\overline{TEC}_m^N$ and $\overline{TEC}^N$ in June are higher in 1999, 2000, and 2004–2008. In other words, the winter anomaly is not found in the mean TEC in all years in the southern hemisphere and in most years in the northern hemisphere.

[23] The monthly mean TEC ($\overline{TEC}_l^G$, $\overline{TEC}_m^G$, $\overline{TEC}_h^G$ and $\overline{TEC}^G$) averaged in both hemispheres show higher values in December than in June during the years 2000 to 2008; that is, the annual anomaly is found in these mean TEC averaged

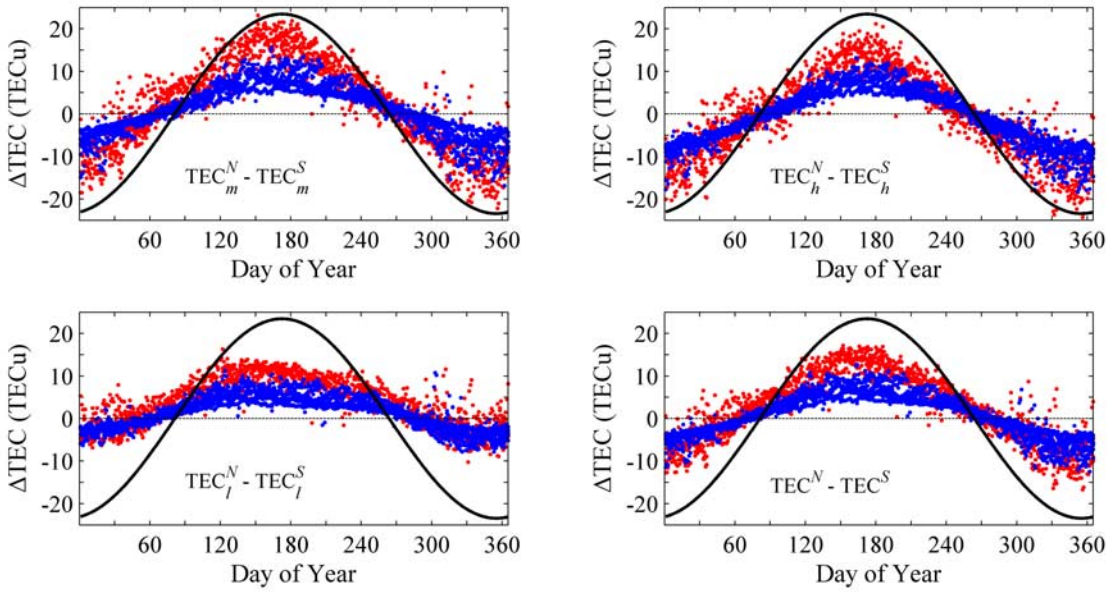

Figure 5. The difference of the daily mean TEC in the northern hemisphere and in the southern hemisphere, averaged at low latitudes (25°–0°), middle latitudes (55°–25°), high latitudes (latitude higher than 55°), and all latitudes (87.5°–0°) as a function of day of year during the years 1999 to 2008. The blue points denote the data when the 1-year moving mean values of $F_{10.7}$ are higher than 140 sfu, while the red ones are for those of $F_{10.7}$ lower than 140 sfu. The curve superimposed in each plot denotes the solar declination. The subscripts *l*, *m*, and *h* stand for low, middle, and high latitude, while the superscripts *N* and *S* stand for the northern and southern hemispheres.

in both hemispheres. An exception is in 1999, when the monthly TEC have higher values in June 1999 than in December 1998 at middle and high latitudes, and the monthly TEC averaged globally and at low latitudes in June 1999 and in December 1998 are of comparable values. It supports the statement that the seasonal anomaly is greater in the northern hemisphere than the southern [*Rishbeth*, 1998]. Figure 4 reveals that the annual anomaly in these mean TEC averaged in both hemispheres becomes more evident at higher solar activity and at low latitudes. Further, these mean TEC can capture the overall picture of the ionosphere in the June and December solstices.

3.4. Hemispheric Asymmetry

[24] Figure 5 plots the differences of the daily mean TEC (averaged globally and over low, middle, and high latitudes as well) in the northern (southern) hemisphere. The red points denote the data when the 1-year running mean values of $F_{10.7}$ are higher than 140 sfu, and the blue points denote the data when the 1-year running mean values of $F_{10.7}$ below 140 sfu.

[25] From Figure 5 one can see that the hemispheric differences in these mean TEC show an annual variation with higher values in the southern (northern) hemisphere near the December (June) solstices, which follow the solar declination as denoted by the thick line. The hemispheric differences become larger at higher solar activity and are stronger at middle and high latitudes than at low latitudes. Moreover, the semiannual component is not obviously detected. This new feature also suggests that (1) the hemispheric differences in these mean TEC are a manifestation of the seasonal variations, mainly due to the annual components with different phases in conjugate hemispheres, and (2) there are strong couplings between both hemispheres in the mechanisms responsible for the semiannual variations in the ionosphere. In other words, there are comparable and in-phase semiannual components in the ionosphere of both hemispheres. As a result, the hemispheric differences leave an absolute annual component.

3.5. Solar Activity Dependence and Solar Rotation Variations of the Mean TEC

[26] The daily mean TEC averaged at three latitude bands in both hemispheres during the years 1998 to 2008 are plotted as a function of the relevant $F_{10.7}$ and the daily mean values of SEM/SOHO solar full disk EUV flux (0.1–50 nm wavelength band) in Figure 6. A piecewise linear regression is applied to show the solar activity dependency of the daily mean TEC for three latitude bands. The thick curve denotes the piecewise fitting results, and the dashed line depicts the result of a linear regression for the lower data part of (the left-hand plots) the values of $F_{10.7} < 180$ sfu or (the right-hand plots) that of EUV (0.1–50 nm) $<5 \times 10^{10}$ photons cm^{-2} s^{-1}, with the equation indicated.

[27] From Figure 6, one can see strong solar activity variations in the daily mean TEC. A linear regression can roughly describe the solar dependency of the daily mean TEC. In more detail, the saturation effect can be found in the mean TEC versus $F_{10.7}$, being more evident at low-latitude mean TEC when $F_{10.7}$ approaches values greater than 200 sfu. The saturation effects at high $F_{10.7}$ have already been reported in NmF2 and TEC [e.g., *Balan et al.*, 1994; *Chen et al.*, 2008; *Liu et al.*, 2003, 2004, 2006; *Richards*, 2001; *Su et al.*, 1999]. It was also founded in

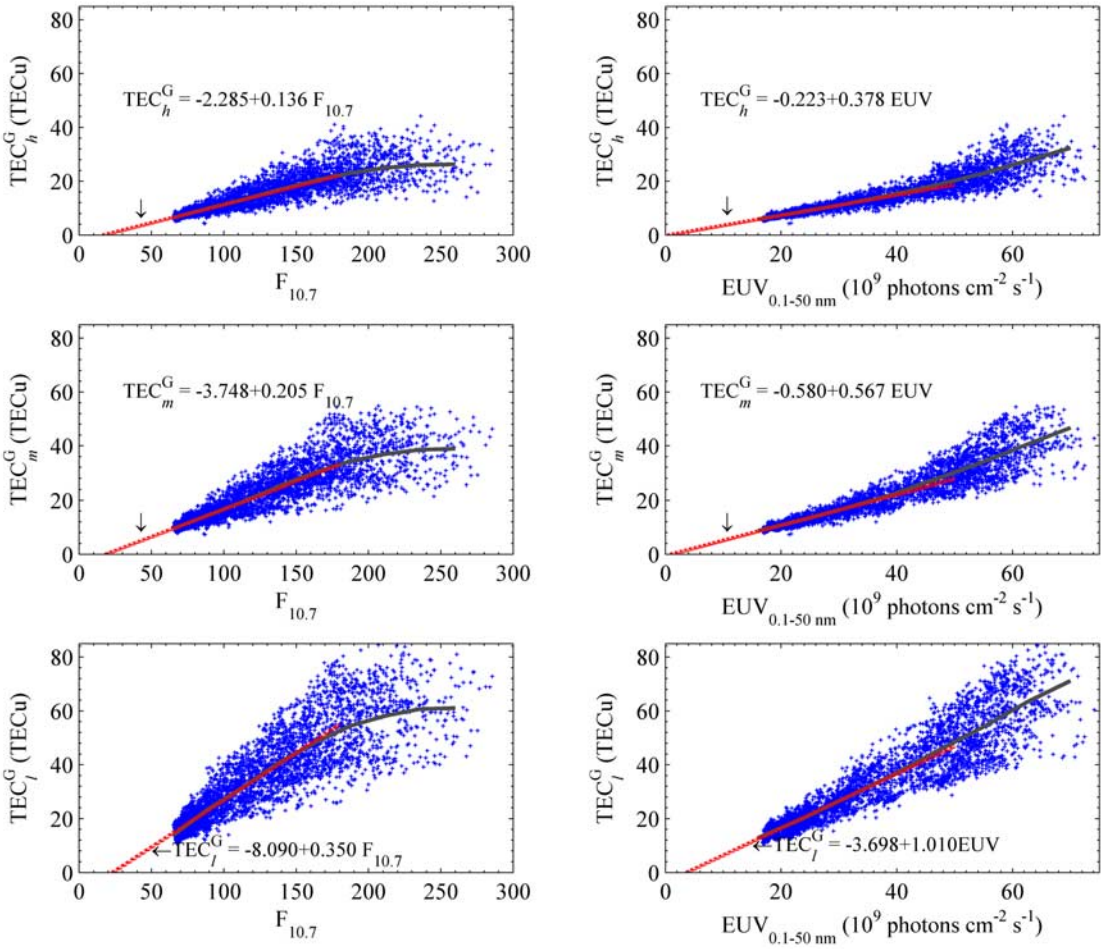

Figure 6. The dependence of the daily averaged values of mean TEC ($\overline{TEC}_l^G$, $\overline{TEC}_m^G$, and $\overline{TEC}_h^G$) on $F_{10.7}$ and SOHO/SEM EUV at the 0.1–50 nm wavelength band in 1998–2008. The daily averages of mean TEC are averaged in both hemispheres at high latitudes (latitude higher than 55°), middle latitudes (55°–25°), and low latitudes (25°–0°). The subscripts *l*, *m*, and *h* stand for low, middle, and high latitude, while the superscript *G* stands for the TEC averaged in both hemispheres. The SOHO/SEM EUV fluxes at the 0.1–50 nm wavelength band are in units of 10^9 photons cm^{-2} s^{-1}. The thick curve denotes the moving linear fit for the data, and the dashed line denotes the linear trend, which is also described by the corresponding equation.

GEC [*Afraimovich et al.*, 2008]. *Liu et al.* [2006] revealed that there are seasonal and latitudinal variations in the solar dependency of NmF2 by examining $F_{10.7}$, solar EUV, and NmF2 from 20 ionosonde stations with the longest historical data series available. They further confirmed the saturation effect in NmF2 versus solar EUV due to the dynamic processes and the close couplings between the ionosphere and the thermosphere. In contrast, an amplification effect has been found in the topside ionosphere [*Liu et al.*, 2007a] and in the nighttime NmF2 [*Chen et al.*, 2008; *Liu et al.*, 2004]. It is interesting that the amplification effect can also be detected in the mean TEC at middle and high latitudes versus SEM/SOHO EUV; that is, the TEC increases faster or at a higher rate with higher solar EUV fluxes. This amplification effect is a novel feature. As a matter of fact, if we check carefully Figure 3 of *Afraimovich et al.* [2008], the amplification effect can be also found, although they just applied a linear fit on GEC versus the solar EUV fluxes. It should be pointed out that this amplification feature needs further data validation with data under higher EUV fluxes due to the moderate solar activity levels of Solar Cycle 23. It is sure that this amplification feature can also be found at the TEC averaged in one hemisphere and those observed over some locations in certain seasons, which we will report separately in a future work. The inconsistent patterns of the mean TEC versus $F_{10.7}$ and solar EUV can be explained in terms of the nonlinear relationship of $F_{10.7}$ versus solar EUV [e.g., *Balan et al.*, 1994; *Liu et al.*, 2006] due to quite different behaviors on short-term variations of solar activity in $F_{10.7}$ and solar EUV. Further, Figure 6 also clearly shows remarkably better correlation of daily values of mean TEC with EUV (0.1–50 nm) than with $F_{10.7}$.

[28] In addition, there is rather scatter in the plots of Figure 6. Part of the scatter could be due to significant day-to-day and annual/semiannual variabilities. Possible sources also come from that the ionosphere is significantly influenced by solar wind/magnetospheric activities and ionospheric transport processes, which are complicated

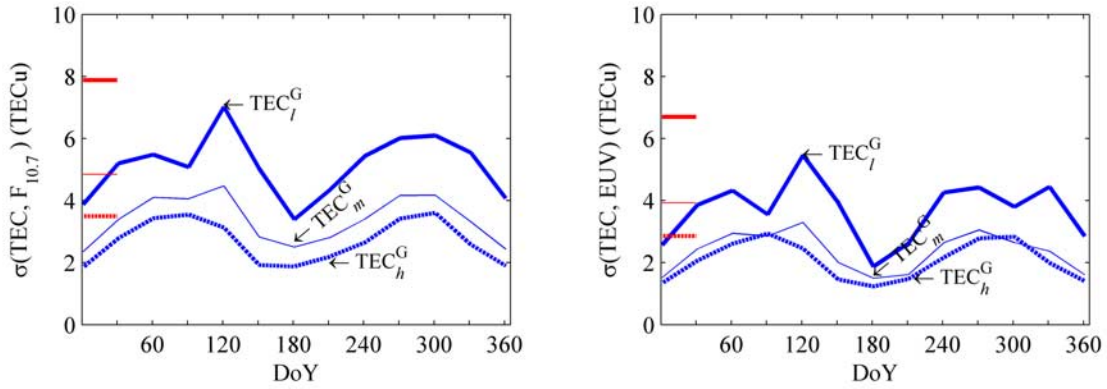

Figure 7. Seasonal variation of the standard deviations of the $\overline{TEC}_l^G$, $\overline{TEC}_m^G$, and $\overline{TEC}_h^G$ predicted with the regression function of $F_{10.7}$ and EUV (0.1–50 nm) from those observed values. The short horizontal bars from the top to the bottom in the left of each plot illustrate those without taking DOY into account.

functions of solar activity. In Figure 6, we used all data regardless of their seasons and geomagnetic conditions. If we separate data according to the months or seasons, the scatter will be decreased to some extent as shown in Figure 7. Figure 7 illustrates the seasonal variation of the standard deviations of the $\overline{TEC}_l^G$, $\overline{TEC}_m^G$, $\overline{TEC}_h^G$ and predicted with the regression function of $F_{10.7}$ and EUV (0.1–50 nm) from those observed values. The short horizontal bars from the top to the bottom on the left hand of each plot illustrate those without taking DOY into account. The standard deviations of those regardless of their seasons and geomagnetic conditions are 7.87, 4.84, and 3.49 TECu for low-, middle-, and high-latitude bands, respectively, in terms of $F_{10.7}$, and 6.85, 4.05, and 2.94 TECu for low-, middle-, and high-latitude bands in terms of EUV (0.1–50 nm). Moreover, the standard deviations are generally smaller if we limited the data in 1–2 month.

[29] Figure 6 also illustrates that the mean TEC sensitivity to solar activity has somewhat latitudinal differences. We applied a linear fit to the data as indicated by the dashed line and the equation gave the derived results over these latitude ranges. The regression slopes as given in the equations decrease with the latitude of the specified ranges, having a highest value at low latitude and a lowest one at high latitude. This latitude difference in solar sensitivity may come from the differences of the solar zenith angle as well as the related parameters (neutral density and concentrations, etc) of the background thermosphere as reported by *Liu et al.* [2006]. As shown in Figure 6, the relationship of those mean TEC with $F_{10.7}$ and EUV (0.1–50 nm) can enough be described in terms of equations given by *Liu et al.* [2004]. Therefore, these mean TEC can be served as ionospheric indices if we separate data according to their months. The errors can be estimated according to the standard deviations shown in Figure 7. Moreover, an interesting point is that the linear regression line has a negative intercept in TEC, which means that when $F_{10.7}$ and EUV approach to zero, the extrapolated ionosphere will have a negative TEC. This feature is consistent with that of the global mean TEC [*Hocke*, 2009]. If carefully checked previous results of the ionosphere [e.g., *Afraimovich et al.*, 2008] and the thermosphere, such as the total neutral density from CHAMP observations [*Liu et al.*, 2005], we can also draw the similar conclusion. Obviously, a negative TEC is unphysical and even if the coronal emission goes to zero, underlying emission should still remain. However, the ionosphere and thermosphere under extreme solar cycle conditions (e.g., the Maunder and Dalton Minima) is quite interesting, which waits for further investigation.

[30] Figure 8 depicts the short-term variations in $F_{10.7}$, SOHO/SEM EUV, and mean TEC at three latitude bands during the years 1999 to 2008. The values shown in Figure 8 are the difference values of the daily mean TEC from the corresponding 54-day running TEC.

[31] The well-known solar rotation variations should modulate the ionosphere as well as the thermosphere. *Rich et al.* [2003] revealed that the 27-day effect is much more pronounced in the topside plasma density. It is possibly masked by the local noises from gravity waves that affect the bottomside ionosphere but not the topside ionosphere. One can see from Figure 8 that the 27-day effects are pronounced in the short-term variations of $F_{10.7}$ and solar EUV as well as in the mean TEC. The 27-day variations of the mean TEC become more effective during the equinoxes, which are consistent with the global pattern of the semiannual variation in the thermospheric O/N_2 [e.g., *Qian et al.*, 2009]. The present result confirms that the ionosphere over different latitudes is strongly modulated with the solar rotation when the noises are greatly depressed by applying an averaging procedure. The mean TEC averaged over three latitude ranges show similar results of the correlation analysis of the GEC during the period of 1999 to 2006 by *Afraimovich et al.* [2008]. Therefore, we do not repeat the analysis here.

4. Summary

[32] This paper has analyzed the 11 years (1998–2008) of data of the GIM TEC derived at JPL to investigate the climatology of the ionosphere and to explore the capability of the mean TEC to track the solar activity variability and capture the overall annual/semiannual variations of the ionosphere over specified latitude ranges. In summary, the major results are outlined as follows.

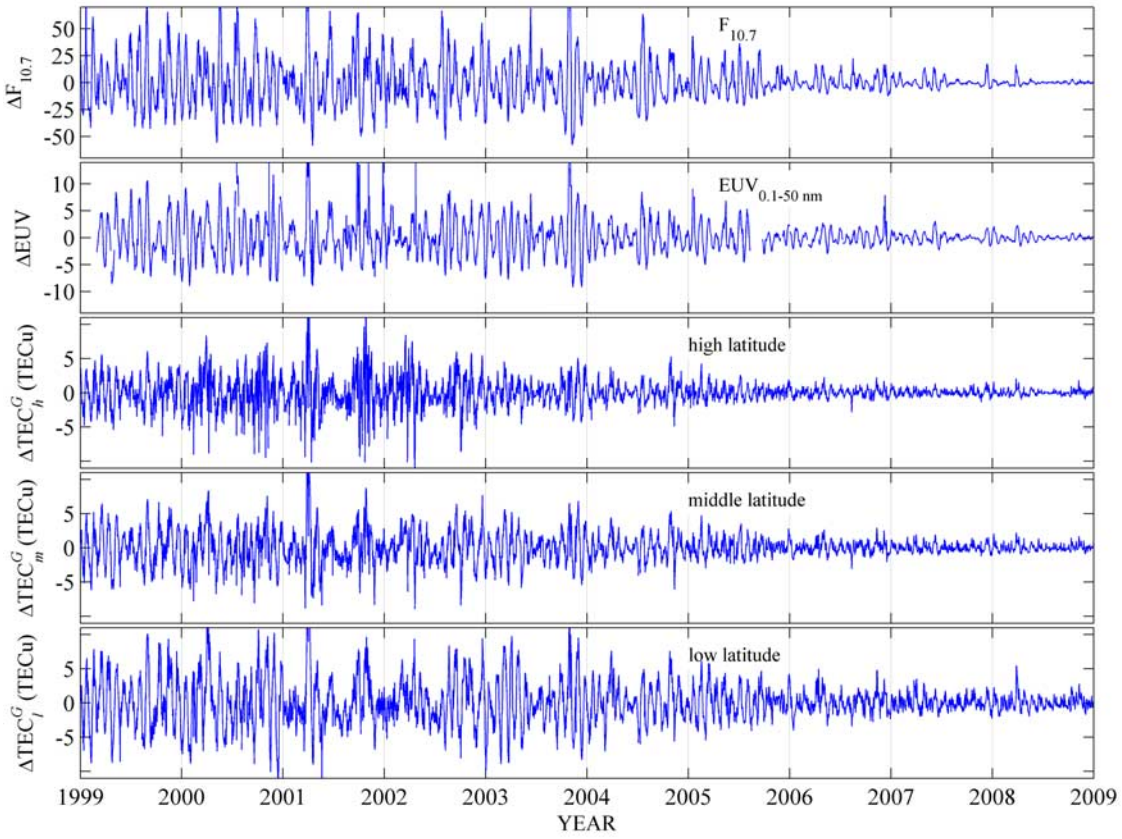

Figure 8. The short-term variations of $F_{10.7}$, SOHO/SEM EUV, and mean TEC at different latitude bands during the years 1999 to 2008. The daily averages of mean TEC are averaged in both hemispheres at all latitudes (0°–87.5°), high latitudes (latitude higher than 55°), middle latitudes (55°–25°), and low latitudes (25°–0°). The subscripts *l*, *m*, and *h* stand for low, middle, and high latitude, while the superscript *G* stands for the TEC averaged in both hemispheres. The SOHO/SEM EUV fluxes at the 0.1–50 nm wavelength band are in units of 10^9 photons cm^{-2} s^{-1}. The values shown are the difference values of the daily mean TEC from the corresponding 54-day running mean TEC. Ticks of year are on 1 January of the years.

[33] 1. The mean TEC averaged globally and at three latitude bands (low, middle, and high latitudes) in one (southern or northern) hemisphere and both hemispheres show strong solar cycle and solar rotation modulations as well as annual/semiannual variations. The averaging procedure can greatly depress the noises, which are partly raised from gravity waves and other processes.

[34] 2. The mean TEC has higher solar activity sensitivity at lower latitude. The saturation effect exists in the mean TEC versus $F_{10.7}$, more evident at low latitudes; while an amplification effect can easily be detected in the mean TEC versus solar EUV at higher latitude. An interesting result is that the TEC will take negative values when the values of $F_{10.7}$ or the solar EUV fluxes extrapolated to zero. Similar feature can also be found in global mean TEC [*Hocke*, 2009], NmF2 [*Liu et al.*, 2006], and neutral total density [*Liu et al.*, 2005]. It stimulates our interest on what the ionosphere and thermosphere will be under extreme solar cycle conditions (the Maunder and Dalton Minima).

[35] 3. The annual component of the mean TEC has greater amplitudes in the southern hemisphere than in the northern hemisphere. The annual phases are relatively stable in the southern hemisphere and shift toward vernal equinox and even December solstice at some times in the northern hemisphere. In contrast, there are in phase and comparable amplitudes of the semiannual components in conjugate hemispheres, which suggests close couplings between conjugate hemispheres. The amplitudes of the annual/semiannual components become more pronounced at low latitude and at higher solar activity.

[36] 4. Annual asymmetry and hemispheric difference can be detected in the mean TEC, more distinct with increasing solar activity. The hemispheric difference follows the solar declination.

[37] 5. All these mean TEC can be used as ionospheric indices to track the solar activity variation due to solar cycle and solar rotation modulations, and the TEC averaged in one (southern or northern) hemisphere will reliably capture the overall features of the ionosphere over specified latitude ranges. However, these TEC averaged in both hemispheres should be used with caution, because the mitigation of annual variations with different phases in conjugate hemisphere may leave a significant semiannual component in these mean TEC. It may provide false information on the

ionosphere, especial at LSA, when the ionosphere is actually dominated with annual variations.

[38] **Acknowledgments.** We greatly thank two reviewers whose detailed suggestions improved the quality of the paper. This research was supported by National Natural Science Foundation of China (40725014, 40674090, 40636032) and National Important Basic Research Project (2006CB806306). The JPL GIMs were downloaded from the site ftp://cddis.gsfc.nasa.gov. The research at JPL, California Institute of Technology, is performed under a contract with the U.S. National Aeronautics and Space Administration. The $F_{10.7}$ index was taken from the SPIDR Web site, and the SOHO/SEM EUV data were taken from the site http://www.usc.edu/dept/space_science/.

[39] Wolfgang Baumjohann thanks Ivan Kutiev and another reviewer for their assistance in evaluating this paper.

References

Afraimovich, E. L., E. I. Astafyeva, A. V. Oinats, Y. V. Yasukevich, and I. V. Zhivetiev (2008), Global electron content: A new conception to track solar activity, *Ann. Geophys.*, *26*, 335–344.

Astafyeva, E. I., E. L. Afraimovich, A. V. Oinats, Y. V. Yasukevich, and I. V. Zhivetiev (2008), Dynamics of global electron content in 1998–2005 derived from global GPS data and IRI modeling, *Adv. Space Res.*, *42*, 763–769, doi:10.1016/j.asr.2007.11.007.

Bailey, G. J., Y. Z. Su, and K.-I. Oyama (2000), Yearly variations in the low-latitude topside ionosphere, *Ann. Geophys.*, *18*, 789–798, doi:10.1007/s00585-000-0789-0.

Balan, N., G. J. Bailey, B. Jenkins, P. B. Rao, and R. J. Moffett (1994), Variations of ionospheric ionization and related solar fluxes during an intense solar cycle, *J. Geophys. Res.*, *99*(A2), 2243–2253, doi:10.1029/93JA02099.

Balan, N., Y. Otsuka, S. Fukao, M. A. Abdu, and G. J. Bailey (2000), Annual variations of the ionosphere: A review based on MU radar observations, *Adv. Space Res.*, *25*(1), 153–162, doi:10.1016/S0273-1177(99)00913-8.

Bowman, B. R., W. K. Tobiska, and M. J. Kendra (2008), The thermospheric semiannual density response to solar EUV heating, *J. Atmos. Sol. Terr. Phys.*, *70*, 1482–1496, doi:10.1016/j.jastp.2008.04.020.

Chen, Y., L. Liu, and H. Le (2008), Solar activity variations of nighttime ionospheric peak electron density, *J. Geophys. Res.*, *113*, A11306, doi:10.1029/2008JA013114.

Duncan, R. A. (1969), *F* region seasonal and magnetic storm behaviour, *J. Atmos. Terr. Phys.*, *31*, 59–70, doi:10.1016/0021-9169(69)90081-6.

Fatkullin, M. N. (1973), Storms and the seasonal anomaly in the topside ionosphere, *J. Atmos. Terr. Phys.*, *35*, 453–468, doi:10.1016/0021-9169(73)90036-6.

Fukao, S., W. L. Oliver, Y. Onishi, T. Takami, T. Tsuda, M. Yamamoto, and S. Kato (1991), *F*-region seasonal behavior as measured by the MU radar, *J. Atmos. Terr. Phys.*, *53*, 599–618, doi:10.1016/0021-9169(91)90088-O.

Fuller-Rowell, T. J. (1998), The "thermospheric spoon": A mechanism for the semiannual density variation, *J. Geophys. Res.*, *103*, 3951–3956, doi:10.1029/97JA03335.

Guo, J., W. Wan, J. M. Forbes, E. Sutton, R. S. Nerem, T. N. Woods, S. Bruinsma, and L. Liu (2007), Effects of solar variability on thermosphere density from CHAMP accelerometer data, *J. Geophys. Res.*, *112*, A10308, doi:10.1029/2007JA012409.

Hedin, A. E. (1991), Extension of the MSIS thermosphere model into the middle and lower atmosphere, *J. Geophys. Res.*, *96*(A2), 1159–1172, doi:10.1029/90JA02125.

Hocke, K. (2008), Oscillations of global mean TEC, *J. Geophys. Res.*, *113*, A04302, doi:10.1029/2007JA012798.

Hocke, K. (2009), Reply to comment by J. T. Emmert et al. on "Oscillations of global mean TEC," *J. Geophys. Res.*, *114*, A01310, doi:10.1029/2008JA013786.

Iijima, B. A., I. L. Harris, C. M. Ho, U. J. Lindqwister, A. J. Mannucci, X. Pi, M. J. Reyes, L. C. Sparks, and B. D. Wilson (1999), Automated daily process for global ionospheric total electron content maps and satellite ocean altimeter ionospheric calibration based on Global Positioning System data, *J. Atmos. Sol. Terr. Phys.*, *61*, 1205–1218, doi:10.1016/S1364-6826(99)00067-X.

Judge, D., et al. (1998), First solar EUV irradiances obtained from SOHO by the SEM, *Sol. Phys.*, *177*, 161–173, doi:10.1023/A:1004929011427.

Kawamura, S., N. Balan, Y. Otsuka, and S. Fukao (2002), Annual and semiannual variations of the midlatitude ionosphere under low solar activity, *J. Geophys. Res.*, *107*(A8), 1166, doi:10.1029/2001JA000267.

King-Hele, D. G., and D. M. C. Walker (1969), Air density at a height of 470 km between January 1967 and May 1968, from the orbit of the satellite 1966-118A, *Planet. Space Sci.*, *17*, 197–215, doi:10.1016/0032-0633(69)90038-5.

Liu, H., H. Lühr, V. Henize, and W. Köhler (2005), Global distribution of the thermospheric total mass density derived from CHAMP, *J. Geophys. Res.*, *110*, A04301, doi:10.1029/2004JA010741.

Liu, J. Y., Y. I. Chen, and J. S. Lin (2003), Statistical investigation of the saturation effect in the ionospheric foF2 versus sunspot, solar radio noise, and solar EUV radiation, *J. Geophys. Res.*, *108*(A2), 1067, doi:10.1029/2001JA007543.

Liu, L., W. Wan, and B. Ning (2004), Statistical modeling of ionospheric foF2 over Wuhan, *Radio Sci.*, *39*, RS2013, doi:10.1029/2003RS003005.

Liu, L., W. Wan, B. Ning, O. M. Pirog, and V. I. Kurkin (2006), Solar activity variations of the ionospheric peak electron density, *J. Geophys. Res.*, *111*, A08304, doi:10.1029/2006JA011598.

Liu, L., W. Wan, X. Yue, B. Zhao, B. Ning, and M.-L. Zhang (2007a), The dependence of plasma density in the topside ionosphere on solar activity level, *Ann. Geophys.*, *25*(6), 1337–1343.

Liu, L., B. Zhao, W. Wan, S. Venkartraman, M.-L. Zhang, and X. Yue (2007b), Yearly variations of global plasma densities in the topside ionosphere at middle and low latitudes, *J. Geophys. Res.*, *112*, A07303, doi:10.1029/2007JA012283.

Liu, L., B. Zhao, W. Wan, B. Ning, M.-L. Zhang, and M. He (2009), Seasonal variations of the ionospheric electron densities retrieved from Constellation Observing System for Meteorology, Ionosphere, and Climate mission radio occultation measurements, *J. Geophys. Res.*, *114*, A02302, doi:10.1029/2008JA013819.

Ma, R., J. Xu, and H. Liao (2003), The features and a possible mechanism of semiannual variation in the peak electron density of the low latitude F2 layer, *J. Atmos. Sol. Terr. Phys.*, *65*, 47–57, doi:10.1016/S1364-6826(02)00192-X.

Mannucci, A. J., B. D. Wilson, D. N. Yuan, C. M. Ho, U. J. Lindqwister, and T. F. Runge (1998), A global mapping technique for GPS derived ionospheric total electron content measurements, *Radio Sci.*, *33*, 565–582, doi:10.1029/97RS02707.

Mayr, H. G., and K. K. Mahajan (1971), Seasonal variation in the F_2 region, *J. Geophys. Res.*, *76*, 1017–1027, doi:10.1029/JA076i004p01017.

Mendillo, M., C. Huang, X. Pi, H. Rishbeth, and R. Meier (2005), The global ionospheric asymmetry in total electron content, *J. Atmos. Sol. Terr. Phys.*, *67*, 1377–1387, doi:10.1016/j.jastp.2005.06.021.

Meza, A., and M. P. Natali (2008), Annual and semiannual TEC effects at low solar activity in midlatitude Atlantic region based on TOPEX, *J. Geophys. Res.*, *113*, D14115, doi:10.1029/2007JD009088.

Millward, G. H., R. J. Moffett, S. Quegan, and T. J. Fuller-Rowell (1996), Ionospheric F_2 layer seasonal and semiannual variations, *J. Geophys. Res.*, *101*, 5149–5156, doi:10.1029/95JA03343.

Oliver, W. L., S. Kawamura, and S. Fukao (2008), The causes of the midlatitude F layer behavior, *J. Geophys. Res.*, *113*, A08310, doi:10.1029/2007JA012590.

Qian, L., S. C. Solomon, and T. J. Kane (2009), Seasonal variation of thermospheric density and composition, *J. Geophys. Res.*, *114*, A01312, doi:10.1029/2008JA013643.

Rich, F. J., P. J. Sultan, and W. J. Burke (2003), The 27-day variations of the plasma densities and temperatures in the topside ionosphere, *J. Geophys. Res.*, *108*(A7), 1297, doi:10.1029/2002JA009731.

Richards, P. G. (2001), Seasonal and solar cycle variations of the ionospheric peak electron density: Comparison of measurement and models, *J. Geophys. Res.*, *106*(A7), 12,803–12,819, doi:10.1029/2000JA000365.

Rishbeth, H. (1998), How the thermospheric circulation affects the ionosphere, *J. Atmos. Sol. Terr. Phys.*, *60*, 1385–1402, doi:10.1016/S1364-6826(98)00062-5.

Rishbeth, H., and I. C. F. Müller-Wodarg (2006), Why is there more ionosphere in January than in July? The annual asymmetry in the F2-layer, *Ann. Geophys.*, *24*, 3293–3311.

Rishbeth, H., I. C. F. Müller-Wodarg, L. Zou, T. J. Fuller-Rowell, G. H. Millward, R. J. Moffett, D. W. Idenden, and A. D. Aylward (2000), Annual and semiannual variations in the ionospheric F2-layer: II. Physical discussion, *Ann. Geophys.*, *18*, 945–956, doi:10.1007/s00585-000-0945-6.

Rüster, R., and J. W. King (1973), Atmospheric composition changes and the *F*2-layer seasonal anomaly, *J. Atmos. Terr. Phys.*, *35*, 1317–1322, doi:10.1016/0021-9169(73)90164-5.

Su, Y. Z., G. J. Bailey, and K.-I. Oyama (1998), Annual and seasonal variations in the low-latitude topside ionosphere, *Ann. Geophys.*, *16*, 974–985, doi:10.1007/s00585-998-0974-0.

Su, Y. Z., G. J. Bailey, and S. Fukao (1999), Altitude dependencies in the solar activity variations of the ionospheric electron density, *J. Geophys. Res.*, *104*(A7), 14,879–14,891, doi:10.1029/1999JA900093.

Titheridge, J. E., and M. J. Buonsanto (1983), Annual variations in the electron content and height of the *F* layer in the northern and southern

hemispheres, related to neutral compositions, *J. Atmos. Terr. Phys.*, *45*, 683–696, doi:10.1016/S0021-9169(83)80027-0.

Torr, M. R., and D. G. Torr (1973), The seasonal behaviour of the *F*2-layer of the ionosphere, *J. Atmos. Terr. Phys.*, *35*, 2237–2251, doi:10.1016/0021-9169(73)90140-2.

Torr, D. G., M. R. Torr, and P. G. Richards (1980), Causes of the F region winter anomaly, *Geophys. Res. Lett.*, *7*, 301–304, doi:10.1029/GL007i005p00301.

West, K. H., R. A. Heelis, and F. J. Rich (1997), Solar activity variations in the composition of the low-latitude topside ionosphere, *J. Geophys. Res.*, *102*(A1), 295–305, doi:10.1029/96JA03031.

Wright, J. W. (1963), The *F* region seasonal anomaly, *J. Geophys. Res.*, *68*, 4379–4381.

Yonezawa, T. (1971), The solar-activity and latitudinal characteristics of the seasonal, non-seasonal and semi-annual variations in the peak electron densities of the *F*2-layer at noon and midnight in middle and low latitudes, *J. Atmos. Terr. Phys.*, *33*, 889–907, doi:10.1016/0021-9169(71)90089-4.

Yu, T., W. Wan, L. Liu, and B. Zhao (2004), Global scale annual and semiannual variations of daytime NmF2 in the high solar activity years, *J. Atmos. Sol. Terr. Phys.*, *66*, 1691–1701, doi:10.1016/j.jastp.2003.09.018.

Zeng, Z., A. Burns, W. Wang, J. Lei, S. Solomon, S. Syndergaard, L. Qian, and Y. Kuo (2008), Ionospheric annual asymmetry observed by the COSMIC radio occultation measurements and simulated by the TIEGCM, *J. Geophys. Res.*, *113*, A07305, doi:10.1029/2007JA012897.

Zhang, S.-R., and J. M. Holt (2007), Ionospheric climatology and variability from long-term and multiple incoherent scatter radar observations: Climatology in eastern American sector, *J. Geophys. Res.*, *112*, A06328, doi:10.1029/2006JA012206.

Zhao, B., W. Wan, L. Liu, X. Yue, and S. Venkatramn (2005), Statistical characteristics of the total ion density in the topside ionosphere during the period 1996–2004 using empirical orthogonal function (EOF) analysis, *Ann. Geophys.*, *23*, 3615–3631.

Zhao, B., W. Wan, L. Liu, T. Mao, Z. Ren, M. Wang, and A. B. Christensen (2007), Features of annual and semiannual variations derived from the global ionospheric maps of total electron content, *Ann. Geophys.*, *25*, 2513–2527.

Zou, L., H. Rishbeth, I. C. F. Muller-Wodarg, A. D. Aylward, G. H. Millward, T. J. Fuller-Rowell, D. W. Idenden, and R. J. Moffett (2000), Annual and semiannual variations in the ionospheric F2-layer: I. Modelling, *Ann. Geophys.*, *18*, 927–944, doi:10.1007/s00585-000-0927-8.

L. Liu, B. Ning, W. Wan, and M.-L. Zhang, Beijing National Observatory of Space Environment, Institute of Geology and Geophysics, Chinese Academy of Sciences, Beijing 100029, China. (liul@mail.iggcas.ac.cn)